Mixing in a T-shaped microreactor: scales and quality of mixing

Dieter Bothe^{a*}, Carsten Stemich^b, Hans-Joachim Warnecke^b

^aChair for Mathematics, Center of Computational Engineering Science, RWTH Aachen, Pauwelsstraße 19, 52074 Aachen, Germany

^bInstitute of Chemical Engineering, Department of Chemistry, Faculty of Sciences, University of Paderborn, Warburger Straße 100, 33098 Paderborn, Germany

The large area-to-volume ratio of microreactors gives prospect of better yield and selectivity than for conventional designs, since diffusive fluxes of mass and heat in micro-devices scale with area, while the rate of changes corresponding to sources and sinks are proportional to volume. Indeed, theoretical considerations of the scaling behaviour (see [1]) support the fact that micro-reactors allow for faster chemical reactions and provide better thermal control. Moreover, specific applications prove that these advantages of micro-reactors can be realised in order to perform fast exothermic reactions (cf. [2-4]) and to enhance selectivity [5].

For such applications, the mixing of chemical species is of special interest, since it is an essential condition for chemical reactions. To obtain efficient mixing for the short residence times in micro-systems, the contact area between regions of higher and lower species concentration has to be increased significantly. To avoid large pressure drops, secondary flows instead of turbulent flow fields are preferred. In case of a T-shaped micro-mixer, the secondary flow acts mainly in cross directions, i.e. perpendicular to the axial direction, and can be used to mix the two feed streams. To assess and optimise the mixing process, this qualitative picture has to be understood more thoroughly and significant quantitative information has to be added. In particular, the interplay of convective and diffusive transport to bridge the gap between the reactor and the molecular scale, have to be further investigated, since even if no new physico-chemical phenomena occur, new aspects enter the picture in case of micro-systems; cf. [6] and the references given there. The present paper employs CFD-simulations to obtain first steps in this direction.

1. Mixing: a multiscale process

Reactive mixing is a multiscale process per se, since educts are usually initially segregated, while mixing on the molecular level is necessary for any chemical reaction to occur. Whatever transport processes are involved on the macro- or meso-scale, the final step to obtain homogeneity on the molecular scale – the so-called micro-mixing – can solely be achieved by molecular diffusion. To avoid adverse effects of imperfect mixing on conversion and selectivity, the total mixing time should be well below the time-scale of chemical reaction. Since typical residence times in micro-channels are significantly smaller than in

^{*} Corresponding author. Tel.: +49-5251-60-3619; Fax: +49-5251-60-3244. Email address: bothe@tc.upb.de.

D. Bothe et al.

macroscopic systems, the contact area between regions of higher and lower species concentration has to be increased considerably in order to advance diffusive dissipation of concentration gradients. An increase of the contact area can either be reached mechanically or hydrodynamically (cf., e.g. [7, 8]). Here, we only consider hydrodynamically driven mixing of liquids.

In continuous processes, mixing in axial direction is often unwanted, since it reduces conversion and strongly influences selectivities. Consequently, mixing should combine complete and instantaneous stirring in cross directions with no

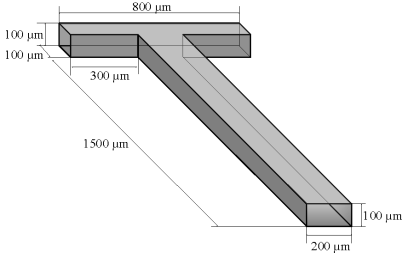


Figure 1. T-shaped micro-mixer.

relative axial movements (plug flow). While this evidently cannot be achieved completely, secondary flows can be employed to approximate such a mixing behaviour. In case of duct-like geometries this leads to T-shaped reactors in the simplest case (cf. Figure 1) or to zigzag-channels with a T-shaped inlet as a more efficient alternative (cf. [8]). Focusing on Tshaped chemical reactors, once the flow

(2)

type, given in terms of the Reynolds number, is fixed, the optimal dimensions of the mixing channel are to a large extent determined by the needed hydrodynamical residence time $\tau_{\rm H}$. Indeed, simple considerations using in particular $\tau_{\rm H}=5\,\tau_{\rm R}$ and $l/d_{_{\rm H}}=10...100$ lead to

$$d_{\rm H} = a \sqrt{\text{Re} \, v \, \tau_{\rm R}}$$
 with $\text{Re} = \frac{U d_{\rm H}}{v}$ and $a = 0.07...0.2$. (1)

In case of a chemical reaction with time-scale $\tau_R = 1$ ms in an aqueous system and a typical Reynolds number of about 200 for engulfment flow (explained below), this leads to a hydraulic diameter in the range of 30...100 μ m.

While scaling considerations give a first hint why microreactors are useful especially for fast chemical reactions [1], they do not answer the question whether cross-directional transport due to secondary flow within a duct of this dimension is fast enough to achieve efficient mixing. In this respect notice first that if the time $\tau_{\rm D}$ available for micro-mixing is estimated as $\tau_{\rm D} = 0.01 \tau_{\rm R}$, in order to avoid limitation by diffusion, then the scale of segregation $l_{\rm S}$ should be reduced to

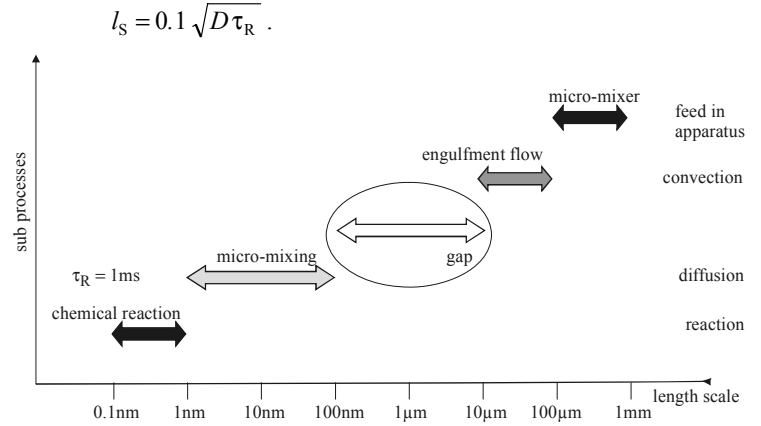


Figure 2. Hierarchy of scales.

This leads to

$$d_{\rm H}/l_{\rm S} = b \sqrt{{\rm Re \, Sc}}$$
 with ${\rm Sc} = v/D$, $b = 0.7...2$ (3)

for the ratio of the initial (maximum) scale of segregation and those needed for micro-mixing to work fast enough. As an example, Re=200 as above and a typical value of Sc=1000 in aqueous systems yield a ratio in the range 300...1000. In other words, by means of the secondary flow, the initial scale on which the feed streams are segregated has to be decreased by a factor of 300...1000 within a small section of the mixing channel. Depending on the structure and effectiveness of the secondary flow, a gap within the hierarchy of scales may remain that should be bridged e.g. by repeated reorientation or by flow modulation to trigger chaotic advection. Figure 2 illustrates this hierarchy of scales for a T-shaped micro-mixer in case of so-called engulfment secondary flow.

2. Numerical simulation of flow and species transport

The numerical simulations presented here are performed for a T-shaped micromixer with rectangular cross sections. The geometry of the micro-reactor consist of two inlet channels, each with a length of 8 mm and a depth of 100 μm . The mixing channel is 16 mm long with the same depth as the inlet channels. The width of the inlet channels are 100 μm each, the width of the mixing channel is 200 μm . For channels of these dimensions and for liquid flow, the transport of mass and momentum is adequately described by the Navier-Stokes equations, which in non-dimensional form read as

$$\nabla \cdot \mathbf{u} = 0$$
, $\partial_{r} \mathbf{u} + \mathbf{u} \cdot \nabla \mathbf{u} = -\nabla p' + \operatorname{Re}^{-1} \Delta \mathbf{u}$, (4)

complemented by appropriate boundary conditions. The transport of an ideally diluted non-reactive chemical species is governed by the species equation

$$\partial_{t} c + \mathbf{u} \cdot \nabla c = (\text{ReSc})^{-1} \Delta c \,, \tag{5}$$

where c denotes the dimensionless molar concentration.

For a reduction of the computational domain, shortened inlet channels and mixing channel are used (Fig. 1). Preliminary calculations gave a minimum length of 1.5 mm for the mixing channel in order to avoid

of perturbations the flow behaviour due to the outflow conditions at this artificial boundary, which only approximate the actual physics. All the results given below refer to a mixing channel length of 1.5 mm and inlet channels with a length of 400 µm. To avoid inlet effects, a fully developed duct flow is used on both inlet faces (cf. [9]). At the



Figure 3. Flow trajectories for engulfment flow (Re=186)

outlet, pressure is set to a fixed reference value and no-slip boundary conditions are used at fixed walls. The numerical simulations were carried out with the CFD software FLUENT 6.2. The computational domain is meshed by a block structured grid of about 1 million cubic grid cells, which is sufficient to resolve

the characteristic features of the flow. For calculations of species concentration for high Schmidt numbers, the mesh is locally refined to resolve the finest scales. The correspondingly modified grid consists of about 12 million cubic grid cells with a local resolution of up to $0.6~\mu m$. The computations are performed with the parallel version of FLUENT using up to 11 processors (64-bit Intel Xeon). The calculations are carried out in the *Paderborn Center for Parallel Computing* (PC²) on the linux-based cluster system ARMINIUS.

3. Intensity and Scale of Segregation

Quantitative measures of the quality of mixing should not only consider the amplitude of the variations present within the concentration distribution, i.e. an intensity of mixing, but also provide a measure for the scale on which gradients persist. For the former, we employ Danckwerts' intensity of segregation [10] defined by

$$I_{\rm S} = \frac{\sigma^2}{\sigma_0^2} \quad \text{with } \sigma^2 = \frac{1}{|V|} \int_V (c - \bar{c})^2 dV \,,$$
 (6)

where \bar{c} denotes the mean value of the concentration field c and $\sigma_0^2 = \bar{c} (c_{max} - \bar{c})$ with feed concentrations zero and c_{max} . Based on (6), we employ

$$I_{\rm M} = 1 - \sqrt{I_{\rm S}} = 1 - \frac{\sigma}{\sigma_0} \,,$$
 (7)

which has a value of 1 in the homogeneously mixed case and 0 for complete segregation. A number of essentially similar measures which depend on statistical parameters are compared in [11].

These measures are insensitive to the length scales on which segregation occurs. To define a meaningful scale of segregation, information about the structure of the concentration distribution is needed. A well-known quantity to characterise the length scale is the striation thickness s. In case of lamellar structures, s^{-1} corresponds to the specific contact area. Given any segregated concentration distribution $c(\mathbf{x})$ inside a volume V, the quantity

$$\Phi(V) = \frac{1}{|V|} \int_{V} ||\nabla f|| dV \quad \text{with} \quad f = \frac{c}{c_{\text{max}}}$$
 (8)

coincides with the specific contact area inside a volume V; here |V| denotes the volume content of V and $||\nabla f||$ is the (Euclidian) length of the gradient of the normalised concentration. Below, we apply an analogous measure to a cross section A instead of a volume V. For a segregated species distribution the quantity Φ then gives the specific contact length inside the cross section. The reciprocal of Φ has the dimension of a length and can be interpreted as an average distance between regions of high and low species concentration. This interpretation is exact in the case of lamellar structures, hence Φ^{-1} is the striation thickness then. The quantity Φ keeps these meanings for almost segregated concentration fields, while these interpretations lose their significance for close to homogeneous fields. In any case, Φ is the *potential for diffusive mixing*, since it measures the total driving force for diffusive fluxes within the concentration field.

The computation of specific contact area or contact line by (8) is also helpful to determine local scales during numerical simulations. Note that if a cross-section contains locally a single tracer filament of width d, then inside an appropriate small part A of that section the filament has length l, i.e. the contact line has length 2l if the contribution of d is negligible. Hence d can be computed as

$$d = 2 \int_{A} f \, dA / \int_{A} ||\nabla f|| \, dA \ . \tag{9}$$

This way, we extract the finest length scales that are present in the simulations below.

4. Flow regimes and mixing

Depending on the mean velocity, three different stationary flow regimes can be observed up to a Reynolds number of about 240, where time-periodic flow phenomena set in. At low Reynolds numbers strictly laminar flow behaviour occurs where both inlet streams run parallel through the mixing channel, without formation of vortices. Above a critical Reynolds number a secondary flow in form of a double vortex pair is build due to centrifugal forces. In this regime, symmetry concerning a plane perpendicular to the inlet channels is still maintained. Therefore, mixing across this symmetry plane can solely occur due to diffusion and, hence, the intensity of mixing is approximately zero. With increasing velocity this flow symmetry is destroyed and fluid elements reach the opposite side of the mixing channel as shown in Figure 3. This so-called engulfment flow regime is the most interesting here, since the resulting intertwinement of both fluid streams generates additional contact area and, hence, raises the potential for diffusive mixing. This causes an increase of the intensity of mixing accompanied by a decrease of the scale of segregation. In fact, as can be seen in Figure 4, these quantities show a jump at the critical mean velocity. Above a mean velocity of approx. 1.1 m/s the scale of segregation, computed from the specific contact area, falls to about 50 µm and further decreases to 30 µm. As mentioned above, these values can be interpreted as a mean distance between regions of high and low tracer concentration. This is

underlined by Figure 5, which shows the tracer distribution on a cross section inside mixing zone, 200 µm from the entrance into the mixing channel. This figure also compares numerical and experimental tracer distribution on a certain cross section inside the mixing channel and thus gives a qualitative validation. The

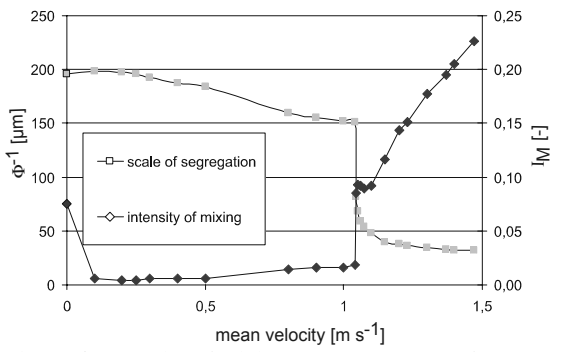


Figure 4. Intensity of mixing (grey) and scale of segregation (black) versus mean velocity.

D. Bothe et al.





Figure 5. Simulated (top) and experimental (bottom) tracer distribution in the mixing channel 200 µm behind its entrance

experimental data is provided by the research group of Prof. Dr. N. Räbiger (IUV, University of Bremen); cf. [12]. The bottom part shows the tracer distribution obtained by laser induced fluorescence combined with micro-resolution confocal microscopy (u-LIF). The top part displays the result of the corresponding numerical simulation with about 9 million grid cells. Both pictures correspond to a mean velocity of 1.4 m/s and are in good agreement. While the computed concentration profile is symmetric with respect to the centre of the cross section, the experimental distribution shows a noticeable might be caused by deviation which asymmetries of the physical channel geometry.

Of course, the size of the finest length scale that occurs depends on the Schmidt number. In the situation of Figure 5, extremely fine structures occur

near the center of both vortices. This is consequence of the high Schmidt number of approx. 3600 of the fluorescence tracer. In the numerical simulation these fine structures are to some extend smeared by numerical diffusion. resolve small scales at relatively large Schmidt numbers of up to 500,

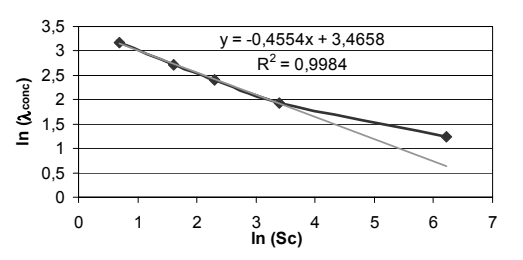


Figure 6. Log-log plot of smallest length scale versus Schmidt number (Re=186).

locally refined grids of up to 18 million cubic grid cells are used with local cell sizes down to $0.6~\mu m$. To investigate how the size of the smallest structures depends on Sc, we performed numerical simulations for different diffusivities and extracted the smallest size by means of (9).

Figure 6 shows the dependence of the smallest scales on Sc at Re=186 and within a cross section at 100 μ m from the entrance of the mixing channel. The first four points correspond to Sc=2, 5, 10, 30 and follow a power law with an exponent of about -0.46. The final point (Sc=500) lies above this curve, most probably due to insufficient grid resolution. Analogous evaluation for Re=173 at the same position also yields a power law dependence with exponent -0.47 again, but with a slightly larger constant which corresponds to a coarser convective scale. It therefore appears that the finest structures λ_{cone} scale as

$$\lambda_{\rm conc} = \lambda_{\rm vel} / \sqrt{\rm Sc} \,\,, \tag{10}$$

where the reference scale λ_{vel} in particular depends on Re. Note that (10) means that the finest scale is given by the Batchelor scale, although the flow

field is even stationary. To build such fine structures requires relative motion accompanied by shear. Since the fine structures are dissipated by diffusion, they can only persist if both sub-processes act on the same time-scale, i.e. if

$$\frac{\lambda_{\text{vel}}^2}{v} = \frac{\lambda_{\text{conc}}^2}{D},\tag{11}$$

which provides a simple explanation for (10).

On the other hand, since the tracer distributions are far from being statistically homogeneous, the average length scale is more important than the smallest one. Somewhat surprisingly, in the engulfment flow regime the mean length scale obtained from the specific contact area scales as

$$\lambda_{\text{conc,av}} = \frac{\lambda_{\text{vel}}}{1 + a \ln(\text{Sc})},$$
(12)

with certain coefficients a = a(Re), in contrast to (10). This has to be further investigated.

5. Acknowledgements

We gratefully acknowledge financial support from the Deutsche Forschungsgemeinschaft within the Priority Program SPP1141 "Analysis, Modelling and Calculation of Mixing Processes with and without Chemical Reaction". We also thank our cooperation partners Prof. Dr. N. Räbiger and Dr. M. Schlüter for providing the experimental data.

References

- [1] D. Bothe, C. Stemich, H.-J. Warnecke, 2006, Fluid mixing in a T-shaped micro-mixer, Chem. Eng. Sci, 61, 2950-8.
- [2] M.-A. Schneider, T. Maeder, P. Ryser, F. Stoessel, 2004, A microreactor-based system for the study of fast exothermic reactions in liquid phase: characterization of the system, Chem. Eng. J., 101, 241-50.
- [3] P. Löb, H. Löwe, V. Hessel, 2004, Fluorinations, chlorinations and brominations of organic compounds in micro reactors, J. Fluorine Chem., 125, 1677-94.
- [4] K. Kawai, T. Ebata, T. Kitazume, 2005, The synthesis of fluorinated materials in microreactors, J. Fluorine Chem., 126, 956-61.
- [5] J. Yoshida, A. Nagaki, T. Iwasaki, S. Suga, 2005, Enhancement of chemical selectivity by microreactors, Chem. Eng. Technol., 28(3), 259-66.
- [6] J.M. Ottino, S. Wiggins, 2004, Introduction: mixing in microfluidics, Phil. Trans. R. Soc. Lond. A, 362, 923-35.
- [7] V. Hessel, H. Löwe, F. Schönfeld, 2005, Micromixers a review on passive and active mixing principles, Chem. Eng. Sci., 60, 2479-2501.
- [8] N.-T. Nguyen, Z. Wu, 2004, Micromixers a review, J. Micromech. Microeng., 15, R1-R16
- [9] D. Bothe, C. Stemich, H.-J. Warnecke, 2004, Theoretische und experimentelle Untersuchungen der Mischvorgänge in T-förmigen Mikroreaktoren – Teil 1: Numerische Simulation und Beurteilung des Strömungsmischens, CIT, 76, 10, 1480-4.
- [10] P.V. Danckwerts, 1952, The definition and measurement of some characteristics of mixtures, Appl. Sci. Res., A3, 279-96.
- [11] J. Boss, 1986, Evaluation of the homogeneity degree of a mixture, Bulk Solids Handlings, 6, 6, 1207-15.
- [12] M. Hoffmann, M. Schlüter, N. Räbiger, 2006, Experimental investigation of liquid-liquid mixing in T-shaped micro-mixers using μ-LIF and μ-PIV, Chem. Eng. Sci, 61, 2968-76.

